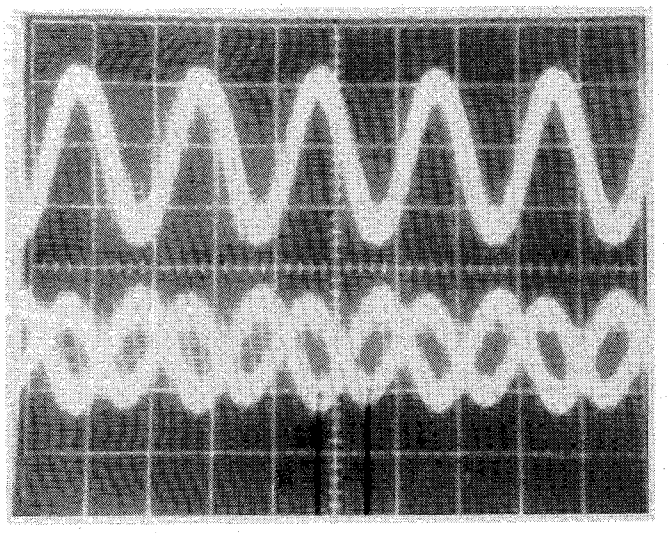

Fig. 4. Two detector outputs, with lower trace showing superimposed phase shifted and unshifted signals through superlattice semiconductor waveguide, 20 ns/div.

shown in Fig. 4. The two traces in the lower channel show both the phase-shifted and unshifted signals incident on the second detector relative to the unshifted signal incident on the first detector. For these data, the phase shift was induced optically by incident argon laser light. A detailed discussion of these superlattice results is provided elsewhere [5].

The optoelectronic approach demonstrated in our work can provide microwave frequency, phase, and amplitude control for many parallel channels in an integrated optical format almost independent of the microwave frequency of interest. This heterodyne approach should also eventually provide microwave frequency and phase hopping on a nanosecond time scale, and has tremendous frequency diversity, as illustrated in Fig. 2.

Acknowledgment

Special thanks go to G. Hasnain of AT&T Bell Labs, Murray Hill, NJ, who provided the selectively contacted doping superlattice samples from his Ph.D. work at the University of California, Berkeley.

References

[1] G. J. Simonis and K. G. Purchase, "Optical generation and distribution of microwave signals," in *Proc. 13th Int. Conf. IR and Millimeter Waves, Proc. SPIE*, vol. 1039, pp. 102–103, 1988.

[2] R. A. Soref, "Voltage-controlled optical/RF phase shifter," *J. Lightwave Technol.*, vol. LT-3, pp. 992–998, 1985.

[3] D. K. Donald, D. M. Bloom, and F. K. David, "Efficient, simple optical heterodyne receiver: DC to 80 GHz," *Optical technology for Microwave Applications II, SPIE*, vol. 545, pp. 29–34, 1985; H. Fettermann, C. Liew, and W. L. Hgai, "Millimeter-visible injection locking and testing," ibid, pp. 26–28.

[4] T. J. Kane and R. L. Byer, "Monolithic unidirectional signal-mode Nd:YAG ring laser," *Opt. Lett.*, vol. 10, pp. 65–67, 1985.

[5] G. J. Simonis and K. A. Purchase, "Optical control of optical phase and amplitude in a doping superlattice waveguide," in *Conf. Lasers and Electro-optics, 1989 Tech. Dig.*, vol. 11, 1989, paper Th J3.

[6] S. Y. Wang and D. M. Bloom, "100 GHz bandwidth planar GaAs Schottky photodiode," *Electron Lett.*, vol. 19, pp. 554–555, 1983.

[7] C. Rauscher, L. Goldberg, and A. M. Yurek, "GaAs FET demodulator for optical–microwave links," *Electron. Lett.*, vol. 22, pp. 705–706, 1986.

[8] M. Tamburrini, M. Parent, L. Goldberg, and D. Stillwell, "Optical feed for a phased array microwave antenna," *Electron. Lett.*, vol. 23, pp. 680–681, 1987.

[9] L. Goldberg, A. M. Yurek, H. F. Taylor, and J. F. Weller, "35 GHz microwave signal generation with an injection-locked laser diode," *Electron. Lett.*, vol. 21, pp. 814–815, 1985.

[10] A. C. Nilsson, E. K. Gustafson, and R. L. Byer, "Eigenpolarization theory of monolithic nonplanar ring oscillators," *IEEE J. Quantum Electron.*, vol. 25, pp. 767–790, 1989.

[11] J. Schlafer, C. B. Su, W. Powaznik, and R. B. Lauer, "20 GHz bandwidth in GaAs photodetector for long-wavelength microwave optical links," *Electron. Lett.*, vol. 21, pp. 469–471, 1985.

[12] Lightwave Electronics Corp., private communication, 1988.

[13] T. Day, E. K. Gustafson, and R. L. Byer, "Active frequency stabilization of a 1.062 μm, Nd:GGG, diode laser pumped nonplanar ring oscillator to less than 3 Hz of relative linewidth," submitted to *Opt. Lett.*

[14] K. J. Williams, R. D. Esman, L. Goldberg, M. Dagenais and J. F. Weller, "Active offset phase locking of Nd:YAG 1319-nm nonplanar ring lasers to 34 GHz," *Electron. Lett*, to be published.

[15] G. Hasnain, C. Chang-Hasnain, A. Dienes, and J. R. Whinnery, "Characteristics of a monolithically integrated doping superlattice optical circuit," *Appl. Phys. Lett.*, vol. 52, pp. 1765–1767, 1988.

Distortion Characteristics of Optical Directional Coupler Modulators

T. R. HALEMANE, MEMBER, IEEE, AND
S. K. KOROTKY, SENIOR MEMBER, IEEE

***Abstract*—Waveguide electro-optic modulators are of much interest for analog optical transmission. Here, a theoretical analysis of the nonlinearities of the intensity modulation response of the optical directional coupler as a function of bias point for the case of phase-mismatch modulation is made and the results are compared with those of interferometric modulators. The interferometric, standard 2×2 directional coupler and the 1×2 y-fed directional coupler modulators are shown to exhibit very similar intermodulation distortion effects. At 4% optical modulation depth, the third-order intermodulation products are −74 dB, −72 dB, and −73.6 dB, respectively, below the carrier level.**

I. Introduction

Electro-optic modulators are intrinsically capable of very high modulation speed and low switching voltage. The optical modulation characteristics of these modulators, i.e., optical intensity output versus applied voltage, are both analog and nonlinear. When used as modulators and switches for digital fiber-optic transmission systems, the nature of the nonlinearity can be used to advantage [1], [2]. However, there is increasing interest in linear analog systems applications. On-ground transmission of satellite communication and radar signals [3]–[5], subcarrier multiplexing techniques [6], laboratory and test instrumentation [7], and sensors are examples where analog modulation with multigigahertz bandwidths would be required. Waveguide electro-optic modulators are also of much interest for multichannel CATV applications because of their potential advantages. These include nearly frequency-independent distortion characteristics, negligible second harmonic distortion if suitably biased, and the ability to increase the output optical power level independent of the modulation depth. The last of these provides the possibility of a larger signal-to-noise ratio and makes it possible to broadcast to several receivers. Additionally, these modulators can exhibit a virtually chirp-free optical spectrum [8] and thereby avoid distortions that might otherwise arise from Fabry–Perot effects created by weak optical reflections within the system.

Manuscript received July 20, 1989; revised November 10, 1989.

The authors are with AT&T Bell Laboratories, Crawfords Corner Road, Holmdel, NJ 07733.

IEEE Log Number 9034523.

Several groups have studied the distortion characteristics of interferometric waveguide modulators [9]–[11]. Measurements of both the second- and third-order nonlinearities are described well by the ideal $\cos^2$ transfer function. These experiments confirm the ability to achieve negligible second harmonic content by adjustment of the dc bias voltage. Recently, similar results have been reported for structures based on the directional coupler [12], [13]. In this paper we examine the theoretical modulation characteristics of the phase-mismatch ($\Delta\beta$) 2×2 and the y-fed 1×2 directional coupler switches with emphasis on the third-order intermodulation distortion.

II. Theory

We consider here an analog optical link based on external modulation of the laser. The electrical signal to be transmitted, denoted V_m, which is implicitly a function of time, drives an electro-optic modulator to produce optical intensity modulation. A square-law detector receives the optical signal and converts it back to an electrical signal. Among the characteristics contributing to the performance of the system are the overall link *electrical* bandwidth, the peak transfer efficiency of electrical RF power from the transmitter to the output of the receiver, and the spurious-free dynamic range. Affecting the dynamic range is the linearity of the modulator. In general, we can express the optical intensity output of the modulator, I, as a function of the applied voltage, V, and input optical intensity, I_o: $I = f(V)I_o$. The photocurrent generated in the detector is proportional to I; thus, if f is linear in V, the output current (voltage) is a replica of the transmitter drive signal.

The waveguide electro-optic modulators achieve amplitude modulation based on modulation of the index of refraction of the waveguide(s) via the electro-optic effect [14]. Potential sources of nonlinear response arise from 1) the electro-optic effect itself; 2) modification of the waveguide characteristics, e.g. propagation loss, because of the index change; and 3) the mechanism used to convert phase modulation to amplitude modulation [19] combined with square-law detection. We believe for Ti:$LiNbO_3$ waveguide electro-optic modulators that the last of the above items is the dominant nonlinear contribution. For example, the ratio of second harmonic power to carrier power attributable to the quadratic electro-optic effect, or Kerr effect, is estimated to be ~ -120 dBc for a modulation depth of 10%. A similar value is estimated for the amount of quadratic modulation arising from a change in propagation loss for well-confining waveguides because of the modification of the real index of the waveguide by the electro-optic effect. We note that in comparison to the index change used to produce Ti:$LiNbO_3$ waveguides for 1.3 μm with low propagation and bending loss ($\sim 10^{-2}$) and the effective index of the corresponding guided mode ($\sim 10^{-3}$), the index change produced by the linear electro-optic effect, or Pockels effect, is less than 10^{-5}. (For waveguides that are weakly confining or have significant loading loss (~ 1 dB/cm) as a result of insufficient buffer layer thickness, the quadratic modulation may not be negligible, however.) Well-confining waveguides will have third-order distortion levels below these second-order values. Consequently, the mechanisms of the third category listed above dominate the third-order intermodulation products, as experiments indicate, and we analyze them here.

The functional form of f depends on the type of waveguide modulator, as discussed below. Both the directional coupler and interferometric modulators are characterized by the minimum voltage swing, V_s, they require to produce 100% modulation depth of the optical intensity. Thus, we anticipate that the modulation characteristic can be expressed in a normalized form:

$$\frac{I}{I_o} = f\left(\frac{V}{V_s}\right). \tag{1}$$

Now, let us assume the modulator is biased at a voltage V_b and also driven by the modulating voltage V_m for a total applied voltage of $V = V_b + V_m$. Anticipating that $V_m \ll V_s$ for linear operation, we consider (1) as a function of V and expand it in a Taylor series about V_b. Then,

$$\frac{I}{I_o}(v) = f(v_b) + \left.\frac{df}{dv}\right|_{v_b} v_m + \frac{1}{2!}\left.\frac{d^2f}{dv^2}\right|_{v_b} v_m^2 + \cdots$$

$$= c_0 + c_1 v_m + c_2 v_m^2 + c_3 v_m^3 + \cdots \tag{2}$$

where

$$v = \frac{V}{V_s} \qquad v_m = \frac{V_m}{V_s} \qquad v_b = \frac{V_b}{V_s}. \tag{3}$$

To evaluate the intermodulation distortion, we consider driving the modulator with two tones under relatively small signal conditions. We take as the modulating voltage

$$V_m = V_o(\sin\omega_1 t + \sin\omega_2 t) = m_t \frac{V_s}{2}(\sin\omega_1 t + \sin\omega_2 t) \tag{4}$$

where we assume the angular frequencies ω_1 and ω_2 satisfy $\Delta \equiv \omega_2 - \omega_1 > 0$ without loss of generality. Here m_t, $0 \leqslant m_t \leqslant 1$, is an input phase modulation index. The second-order term in (2) generates terms at frequencies Δ, $2\omega_1$, $2\omega_1 + \Delta$, and $2\omega_2$. The third-order term contributes to power at several frequencies, including $\omega_1 - \Delta$, ω_1, ω_2, and $\omega_2 + \Delta$, that are in the region of the carrier frequencies and are potential sources of interference.

The optical modulation depth m_o is defined by

$$m_o \equiv \frac{I_{\max} - I_{\min}}{I_{\max} + I_{\min}} \simeq \left|\frac{c_1 V_o}{c_0 V_s}\right| = \left|\frac{c_1}{c_0}\right| \frac{m_t}{2}. \tag{5}$$

This relation between the modulation index of the input electrical signal and the modulation depth of the optical signal output from the modulator depends on the linear coefficient c_1 and the intensity (normalized) c_0 at the bias point and is valid in the small-signal approximation.

When the light falls on a photodetector, the current produced is proportional to the light intensity. Hence, the electrical powers produced by the receiver at the carrier frequency (P_c) and at the second- and third-order intermodulation frequencies (P_{2IM} and P_{3IM}) are related by

$$\frac{P_{2IM}}{P_c} = \frac{c_2^2 c_0^2}{c_1^4} m_0^2 \quad \text{and} \quad \frac{P_{3IM}}{P_c} = \frac{9}{16}\frac{c_3^2 c_0^4}{c_1^6} m_0^4. \tag{6}$$

We note that if the drive power (P_m) is normalized to that required for complete switching (P_s), we obtain

$$\frac{P_m}{P_s} = \frac{V_o^2}{(V_s/2)^2} = m_t^2.$$

The third-order intercept (TOI) is defined as the operating point where P_{3IM} equals P_c when extrapolated from the small-signal regime. From (6), the optical modulation depth at the TOI is given by

$$m_0 = \sqrt{\frac{4}{3}\frac{c_1^3}{c_3 c_0^2}}.$$

The TOI may be expressed in terms of absolute drive voltage (V_s) or power required (P_s) for complete modulation as

$$P_{\mathrm{TOI}} = \frac{16}{3}\left|\frac{c_1}{c_3}\right| P_s \quad \text{and} \quad V_{\mathrm{TOI}} = \sqrt{\frac{16}{3}\left|\frac{c_1}{c_3}\right|}\,\frac{V_s}{2}.$$

To calculate the dynamic range, we assume that the minimum detectable signal is limited by the shot noise. Using the average dc power P_{dc}, which is due to the dc term in (2), the minimum detectable voltage V_{min} is given by

$$\frac{(P_c)_{\mathrm{min}}}{P_{\mathrm{dc}}} = \frac{P_{\mathrm{noise}}}{P_{\mathrm{dc}}}$$

i.e.,

$$\frac{c_1^2 V_{\mathrm{min}}^2}{2c_0^2 V_s^2} = \frac{2qB}{i_{\mathrm{avg}}}$$

or

$$V_{\mathrm{min}} = \left(\frac{4qB}{i_{\mathrm{avg}}}\,\frac{c_0^2 V_s^2}{c_1^2}\right)^{1/2}$$

where i_{avg} is the average photocurrent, q is the electron charge, and B is the receiver bandwidth. The upper limit defining a spurious-free dynamic range is set by the driving voltage which produces an intermodulation distortion term just at the shot noise level. So V_{max}, the maximum spurious-free input voltage, is given by

$$\frac{(P_{3\mathrm{IM}})_{\mathrm{max}}}{P_{\mathrm{dc}}} = \frac{P_{\mathrm{noise}}}{P_{\mathrm{dc}}}$$

i.e.,

$$\frac{9}{32}\,\frac{c_3^2 V_{\mathrm{max}}^6}{c_0^2 V_s^6} = \frac{2qB}{i_{\mathrm{avg}}}$$

or

$$V_{\mathrm{max}} = \left(\frac{64qB}{9i_{\mathrm{avg}}}\,\frac{c_0^2 V_s^6}{c_3^2}\right)^{1/6}.$$

Then, the spurious-free dynamic range (SFDR) is

$$SFDR = \frac{V_{\mathrm{max}}}{V_{\mathrm{min}}} = \left(\frac{2i_{\mathrm{avg}}}{qB}\right)^{1/3}\left(\frac{c_1^3}{6c_0^2 c_3}\right)^{1/3}.$$

A. Interferometric Modulator

The y-branch interferometric modulator consists of waveguides forming two Y junctions in an electro-optic material with coplanar electrodes over the waveguides. The voltage response of the interferometric modulator is described by

$$\frac{I}{I_o} = \cos^2\frac{\Delta\beta L}{2} = \frac{1}{2}\left[1+\cos\pi\frac{V}{V_s}\right]. \tag{7}$$

Here $\Delta\beta L = \pi V/V_s$ corresponds to the electro-optically induced relative phase difference between the two beams. V_s is the minimum voltage required to extinguish the optical output (i.e., $I = 0$). Thus, $f(v) = (1/2)[1+\cos\pi v]$. The derivatives of this function are easily computed. The normalized values of the coefficients c_1, c_2, and c_3 are plotted in Fig. 1 as a function of bias voltage. We observe that the quadratic coefficient, c_2, is identically zero at $v_b = 0.5$. In fact, for the bias point $v_b = 0.5$, we have $c_1 = -\pi/2$, $c_2 = 0$, and $c_3 = \pi^3/12$. Note, too, that c_2 changes sign at that point, which may be used advantageously to cancel any other sources of quadratic modulation if present. When biased at $v_b = 0.5$, the third-order intermodulation product is $P_{3\mathrm{IM}}/P_c = -74.0$ dBc for 4% optical modulation depth. The TOI is 1.80 ($V_s/2$) and is independent of bias. The SFDR is 1.00 $(2i_{\mathrm{avg}}/qB)^{1/3}$ for the bias point $v_b = 0.5$, corresponding to the point of maximally linear response.

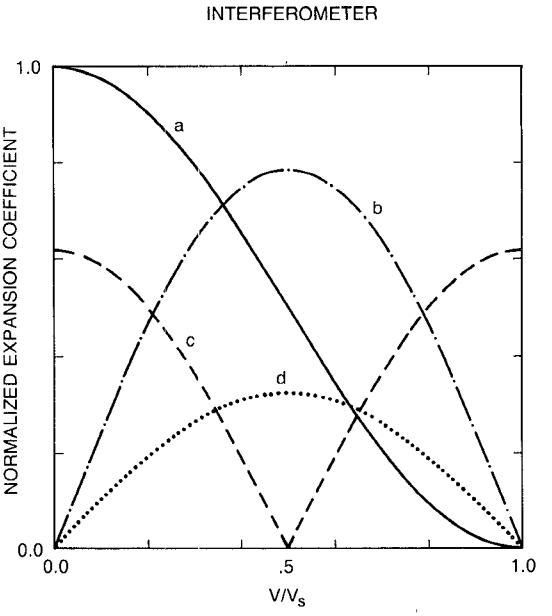

Fig. 1. Switching curve (marked a) and normalized expansion coefficients $|c_1|/2$, $|c_2|/4$, and $|c_3|/8$ (marked as curves b, c, and d) for the interferometric modulator as a function of the normalized bias voltage.

B. Directional Coupler Modulator

Typically, switching in the directional coupler is accomplished by introducing a uniform relative phase velocity difference or mismatch, $\Delta\beta$, between the two waveguides forming the coupler [15]. We let I_0 denote the intensity of light input to one of the coupler inputs and take I_1 and I_2 to denote the intensities at the coupler crossover and straight-through outputs. The response of the coupler is then given by

$$I_2 = \frac{\sin^2\left(\kappa L\sqrt{1+(\delta/\kappa)^2}\right)}{1+(\delta/\kappa)^2} I_0 \quad \text{and} \quad I_1 = I_0 - I_2. \tag{8}$$

Here, κ is the optical coupling coefficient and $\delta \equiv \Delta\beta/2 = \pi\Gamma N^3 r V/2g\lambda$, where N is the effective index of the optical guided mode, r is the electro-optic coefficient, V is the voltage applied between the electrodes, which are separated by a gap g, Γ is the overlap coefficient of the optical and electric fields ($\Gamma \approx 0.25$), and λ is free-space wavelength. Equation (8) can be rewritten to explicitly show the dependence on the applied voltage. We have

$$f(v) = \frac{I_2}{I_0} = \frac{\sin^2\left[\kappa L\sqrt{1+\dfrac{3V^2}{V_s^2}}\right]}{1+\dfrac{3V^2}{V_s^2}}$$

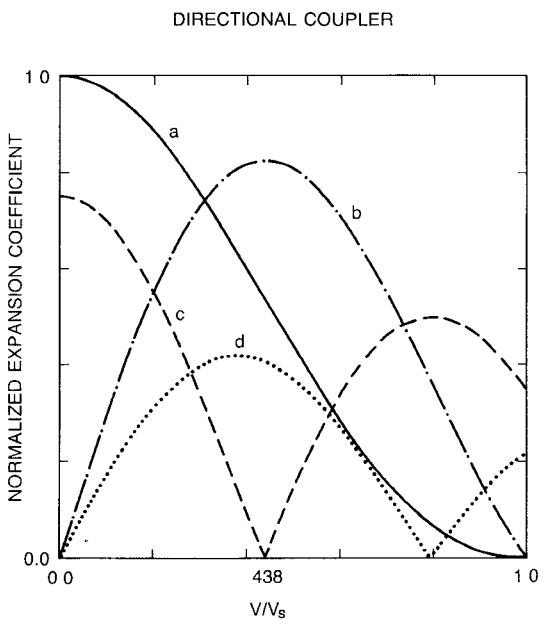

Fig. 2. Switching curve (marked a) and normalized expansion coefficients $|c_1|/2$, $|c_2|/4$, and $|c_3|/8$ (marked as curves b, c, and d) for the directional coupler as a function of the normalized bias voltage.

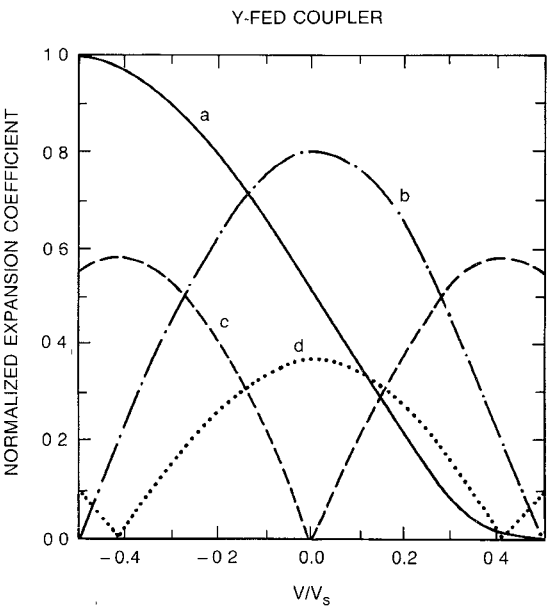

Fig. 3. Switching curve (marked a) and normalized expansion coefficients $|c_1|/2$, $|c_2|/4$, and $|c_3|/8$ (marked as curves b, c, and d) for the y-fed coupler as a function of the normalized bias voltage

where

$$\frac{V_s^2}{3} = \frac{4\kappa^2 g^2 \lambda^2}{\pi^2 \Gamma^2 N^6 r^2}.$$

For complete energy transfer from guide 1 to guide 2, i.e., $I_1 = 0$ at $V = 0$, the requirement on the product κL is in general $\kappa L = (2m+1)\pi/2$. We consider the usual case of $\kappa L = \pi/2$, corresponding to the device of shortest length for a given κ. The voltage V_s then represents that voltage required to switch from the crossover ($I_2 = I_0$) to straight-through ($I_2 = 0$, $I_1 = I_0$) states.

The derivatives of f and, hence, the coefficients c_1, c_2, and c_3 for the directional coupler appearing in the expansion (2) have been calculated. Fig. 2 is a plot of the normalized values of the c_1, c_2, and c_3 coefficients as a function of the normalized bias voltage v_b.

As expected, at zero bias the zeroth- and second-order terms are maximum while the first- and third-order terms are zero. When the bias is $v_b \approx 0.44$, the first-order term is maximum and the second-order term is zero. (Note, as with the interferometer, c_2 changes sign at this point.) This is the point of maximally linear response. At this bias point, the major nonlinear effect is due to the third-order coefficient, c_3. For the bias voltage $V_b \approx 0.44V_s$, we have $c_1 = -1.65$, $c_2 = 0$, $c_3 = 3.23$, and $f(v_b) = 0.54$. We have $P_{3IM}/P_c = -72.0$ dBc for 4% optical modulation depth. The TOI is 1.65 ($V_s/2$) for the bias point chosen, and the SFDR is calculated to be 0.93 $(2i_{avg}/qB)^{1/3}$.

C. y-Fed Coupler Modulator

In the y-fed coupler [16], also called the 1×2 directional coupler, a single-mode input waveguide splits into two symmetrical, coupled waveguides before separating again into two isolated output ports. Modulation is accomplished by applying the modulating voltage at the electrodes placed in the region of the coupler. The general solution for the normalized optical power from the top arm is [12], [16]

$$f(v) = \frac{I}{I_o} = a^2 \cos^2\left(\frac{\pi r}{2}\right) + [(ax - by)/r]^2 \sin^2\left(\frac{\pi r}{2}\right)$$

where $x = \Delta\beta L/\pi$, $y = L/l$, $r^2 = x^2 + y^2$, L is the length of the electrodes, l is the coupling length, $\Delta\beta$ is the induced phase mismatch, and a^2 and b^2 are the power fractions in the top and bottom arms at the input to the coupler. We consider the case of symmetric branching ($a^2 = b^2 = 0.5$). The most linear response is at zero applied voltage. The maximum modulation occurs when $y = 1/\sqrt{2}$. We normalize the voltage so that $v = V/V_s = x/\sqrt{2}$ has the range $(-0.5, 0.5)$ while the intensity in the upper guide switches from maximum to zero.

The derivatives of f with respect to v and hence the coefficients c_1, c_2, and c_3 have been calculated and are plotted in Fig. 3. At zero bias, the first-order term, c_1, is maximum and c_2 is zero. This is the point of maximally linear response. At this point, $c_0 = 0.5$, $c_1 = -1.61$, $c_2 = 0$, and $c_3 = 2.89$. Then, for zero bias, we have $P_{3IM}/P_c = -73.6$ dBc for 4% optical modulation depth. The TOI is 1.72 ($V_s/2$) for the bias point chosen, and the SFDR is calculated to be 0.987 $(2i_{avg}/qB)^{1/3}$.

III. Summary

We find the uniform $\Delta\beta$ switched directional coupler and the y-fed coupler to have distortion characteristics nearly identical to those of interferometric modulators (3IM ~ −74 dBc at 4% modulation depth; see Table I for a list of coefficients). As the distortion characteristics of all three types of modulators analyzed here are similar, other considerations may influence the preferred structure. For example, the use of the external modulator transmitter in a broadcast mode could significantly reduce the system cost, which makes the ability to operate at high optical power levels desirable. In this situation the relative sensitivity to photorefractive phenomena [17] may play a role in determining the waveguide structure of choice. Experiments on Ti:$LiNbO_3$ directional couplers have shown that at optical power levels of 20 mW within a waveguide at $\lambda = 1.3$ μm, the photorefractive phenomenon can act to modify the transfer function, $f(V)$, from its ideal form [17]. Although this does not necessarily imply poor

TABLE I
THE COEFFICIENTS c_0, c_1, c_2, AND c_3 IN THE TAYLOR SERIES EXPANSION FOR THE INTERFEROMETRIC (INT), STANDARD 2×2 DIRECTIONAL COUPLER (DC), AND THE 1×2 y-FED DIRECTIONAL COUPLER (Y-FED) FOR THE BIAS POINT CORRESPONDING TO MAXIMALLY LINEAR RESPONSE $c_2 = 0$

MOD TYPE	BIAS POINT V/V_π	COEFFICIENT c_0	c_1	c_2	c_3	P_{3IM} (dBc) · 4% OMD
INT	0.5	0 5	-1.57	0	2.58	-74.0
DC	0 439	0 536	-1.65	0	3.23	-72.0
Y-FED	0.0	0.5	-1.61	0	2.89	-73.6

Also given is the power at each of the third-order intermodulation frequencies relative to the power at the carrier frequency for 4% optical modulation depth

performance, the y-fed Ti:$LiNbO_3$ waveguide modulator structures offer the potential of operating to significantly higher optical power levels. These structures launch and maintain nearly equal time-averaged optical powers into both waveguides. The y-fed directional coupler and the y-fed interferometer employing a 3 dB coupler (in place of the y-combiner of a standard interferometer) at the output have the further advantage that two signals are immediately available for transmission.

ACKNOWLEDGMENT

The authors wish to thank R. de Ridder for many fruitful discussions.

REFERENCES

[1] S. K. Korotky *et al.*, "8 Gbit/s transmission experiment over 68 km of optical fiber using a Ti:$LiNbO_3$ external modulator," *J. Lightwave Technol.*, vol. LT-5, p. 1505, 1987
[2] R. S. Tucker *et al.*, "16 Gb/s fiber transmission experiment using optical time-division multiplexing," in *Tech. Dig., Conf. Opt. Fiber Commun.* (New Orleans), 1988, paper ThB2
[3] J. E. Bowers, A. C. Chipaloski, S. Boodaghians, and J. W. Carlin, "Long distance fiber optic transmission of C-band microwave signals to and from a satellite antenna," *J. Lightwave Technol.*, vol. LT-5, p. 1733, 1987.
[4] H. Blauvelt, J. Parsons, D. Lewis, and H. Yen, "High-speed GaAs Schottky barrier photodetectors for microwave fiber-optic links," in *Proc. Conf. Opt. Fiber Commun.* (New Orleans), 1984, paper TuH3.
[5] I. L. Newberg, C. M. Gee, G. D. Thurmond, and H. W. Yen, "Radar applications of *X*-band fiber optic links," in *IEEE MTT-S Int. Microwave Symp. Dig.* (New York), 1988, p. 987.
[6] T. E. Darcie, "Subcarrier multiplexing for multiple-access lightwave networks," *J. Lightwave Technol.*, vol. LT-5, p. 1103, 1987.
[7] D. W. Dolfi, M. Nazarathy, and R. L. Jungerman, "Wide-bandwidth 13-bit Barker code $LiNbO_3$ modulator with low drive voltage," in *Proc. Opt. Fiber Commun. Conf.*, 1988, p. 144.
[8] F. Koyama and K. Iga, "Frequency chirping in some types of external modulators," *J. Lightwave Technol.*, vol. 6, p. 87, 1988.
[9] C. H. Bulmer and W. K. Burns, "Linear interferometric modulators in Ti:$LiNbO_3$," *J. Lightwave Technol.*, vol. LT-2, p. 512, 1984.
[10] W. E. Stephens and T. R. Joseph, "System characteristics of direct modulated and externally modulated RF fiber-optic links," *J. Lightwave Technol.*, vol. LT-5, p. 380, 1987.
[11] B. H. Kolner and D. W. Dolfi, "Intermodulation distortion and compression in an integrated electro-optic modulator," *Appl. Opt.*, vol. 26, p. 3676, 1987.
[12] M. McWright Howerton, C. H. Bulmer, and W. K. Burns, "Linear 1×2 directional coupler for electromagnetic field detection," *Appl. Phys. Lett.*, vol. 52, p. 1850, 1988.
[13] G. E. Bodeep and T. E. Darcie, "Comparison of second and third order distortion in intensity modulated InGaAsP lasers and $LiNbO_3$ external modulator," in *Proc. Conf. Opt. Fiber Commun.* (Houston), 1989, paper WK2.
[14] I. P. Kaminow, *An Introduction to Electrooptic Devices*. New York: Academic Press, 1974.
[15] S. K. Korotky and R. C. Alferness, "Waveguide electrooptic devices for optical fiber communication," in *Optical Fiber Telecommunications*, vol. II, S. E. Miller and I. P. Kaminow, Eds. New York: Academic Press, 1988.
[16] S. Thaniyavarn, "Modified 1×2 directional coupler waveguide modulator," *Electron. Lett.*, vol. 22, p. 941, 1986.
[17] G. T. Harvey, "The photorefractive effect in directional coupler and Mach-Zehnder $LiNbO_3$ optical modulators at a wavelength of 1.3 μm," *J. Lightwave Technol.*, vol. LT-6, p. 872, 1987.

Novel Wide-Bandwidth Matching Technique for Laser Diodes

A. GHIASI AND A. GOPINATH, FELLOW, IEEE

***Abstract*—This paper describes a low-loss microstrip matching circuit with large bandwidth for connecting a laser diode of nominal impedance of 2 Ω to a 50 Ω system. The technique utilizes a microstrip Chebyshev transformer without very wide line widths to obtain the match at a center frequency of 10.5 GHz with a bandwidth of 9 GHz, an insertion loss of less than 1.5 dB, and a reflection coefficient of better than −10 dB.**

I. INTRODUCTION

High-speed optical modulation of laser diodes is currently of interest in optically controlled phased array radar [1], and in high-speed optical communications systems. As the modulation frequency extends into the upper microwave and millimeter-wave frequencies, the need arises for an efficient wide-band matching circuit for the laser diode. Currently, the technique used to match the laser diode to a 50 Ω system is to introduce a series resistance to bring up the total termination impedance to 50 Ω. In the case of the Ortel SL1000, the laser is usually modeled by a 2 Ω resistance [2]; thus, the series resistance is 48 Ω. The power delivered to the laser diode is only 4% of the input drive, which is a large loss of power. This paper presents a wide-bandwidth matching circuit with lumped and distributed elements for low-

Manuscript received July 24, 1989; revised November 16, 1989. This work was supported by the Solid State Electronics Division, RADC, Hanscom Field AFB, MA

The authors are with the Department of Electrical Engineering, University of Minnesota, Minneapolis, MN 55455

IEEE Log Number 9034520